23rd ABCM International Congress of Mechanical Engineering
December 6-11, 2015, Rio de Janeiro, RJ, Brazil

ANALYSIS OF NONLINEAR DYNAMICS USING ELECTRONIC CIRCUITS

Guênia Mara Vieira Ladeira
Mechanical Engineering, University Federal of Uberlândia.
e-mail: guenia@mecanica.ufu.br

Gabriela Vieira Lima
Electrical Engineering, University Federal of Uberlândia.
e-mail: gabriela@eel.ufu.br

Cleudmar Amaral Araújo
Mechanical Engineering, University Federal of Uberlândia.
e-mail: cleudmar@mecanica.ufu.br

Abstract. *The essence of chaotic dynamics can be substantially reproduced through analogical electronic systems. Therefore, this article presents the design project of an electronic system based on the mathematical equation of dynamic systems, as well as its responses and analyses of the results. Electronic systems generate the analysis of dynamic behaviour, providing the ease at which it varies the input parameters. In this article, the behaviour of a Duffing Oscillator with characteristics of linear until chaotic is scrutinized. The responses given by the electronic system are compared to the numeric solution produced by the mathematical model of the oscillator. The results from the theoretical and experimental systems were analysed through linear and nonlinear techniques, where it was noted that the experimental system produces adequate results and can be used in the experimental part of teaching nonlinear dynamics as well as for research tests.*

Keywords: dynamic chaotic, analog electronic, experimental analysis.

1. INTRODUCTION

Nonlinear behavior is inherent to a variety of systems, including systems of a biological nature as found in the growth of populations or the functioning of organs in living organisms. In the scope of physics concerning pendulous systems, the orbits of planets affected by several gravitational forces, in engineering, mechanical and electrical systems that possess components and materials of a nonlinear nature. In engineering, this behavior has been studied under the motivation of eliminating nonlinearity or to use the variety in behavior to optimize its operation.

According to Ogata (2004), dynamic systems electrical and mechanical can produce analogous responses, represented by the same mathematical model; these systems are described through equations with the same derivatives or integrals. Experimental mechanical systems are difficult to implement, due to the high cost associated with the equipment. In most cases, the research and teaching of dynamics is limited to simulations by computer analysis, which means that responses are limited to mathematical theory, and to interference and noise that is already common knowledge. This therefore means that, other interferences and noises aggregated from real systems do not contribute to the simulation. Experimental systems also becoming an easier and more interesting form for analyzing behavior.

In this study, the authors present a behavioral analysis of the nonlinear Duffing Oscillator. The software Matlab® was employed to resolve the mathematical function of the system through numerical methods, as well as the response analysis of the experimental system. Time series analysis of some interesting responses are analyzed in both time and frequency, with the Poincare section being constructed for highlighted responses. The reconstruction parameters of the state spaces are also analyzed, the minimum dimension of immersion, time delay and the behavior of the higher Lyapunov exponent.

The authors also simulated the project for the electric circuit through a suitable program and the data were analyzed. The analogy of the experimental system and the construction of the circuit are explained for the purpose of reconstruction. After the application of adjusts, the experimental circuit was once again solved through numerical methods in order to compare the results.

2. DUFFING OSCILLATOR

According to Tamaseviciute *et al*. (2008), the oscillation equation with cubic rigidity from the Duffing Oscillator can be used to describe the dynamics of an electrical or mechanical system. The Duffing system can be represented by Fig.1, containing mass, nonlinear spring and dampening. Thus, possessing as characteristic the variable B that represents the parameter of nonlinearity relative to the rigidity of the spring, in accordance with Eq.1 and in this system consisting of an external excitation force.

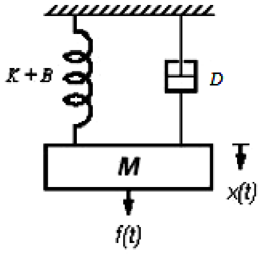

$$M\ddot{x} + D\dot{x} + Kx + Bx^3 = f\,cos\,(\omega t) \tag{1}$$

Figure 1 - Model of physical system

3. ELECTRONIC CIRCUIT DUFFING OSCILLATOR

3.1 Project electronic circuit

Electrical circuits can act as integrator or derivator, multiplier or divider, adder or subtractor, among many other possibilities. These circuits are based on amplifier operations and for each operation there exists a special construction procedure (Malvino, 1995). The composition of the electronic prototype can be used for the analysis of the system's behavior and the adjustment of those parameters for response control.

In order to solve the Duffing Oscillator equation, the authors developed an electronic system, which contains analogical integrators and multipliers.

The electronic circuit integrator converts the input signal in accordance with Eq.2, where it is noted that the RC time constant integration should present a low value in order that the circuit stabilizes quickly. This is due to the fact that the before the circuit acts as an integrator, the capacitors need to be loaded according to the initial conditions. In a seemingly counterintuitive manner, it is also necessary to consider that in the RC project needs to be greater than ten times the signal period, i.e. RC > 10T.

$$y(t) = \frac{1}{RC}\int_0^t x(t)dt \tag{2}$$

When the integrated circuit is excited by an alternated signal there exists an inversely proportionate gain to the frequency, as in Eq.3. Therefore, verifying that the circuit is insensitive to high frequency noise and in low frequencies, the gain is considerably incremented, tending towards infinity when the frequency tends towards zero.

$$A = \frac{1}{2\pi fRC} \tag{3}$$

Whereas, the multiplication of a sinusoidal signal by itself generates a DC level and an alternated signal with double the frequency, as shown in Eq.4. And, following on with a second multiplication generating a component with three times the excitation frequency, as well as an initial frequency component, in accordance with Eq.5 the multiplier circuit is suitable for producing x^3.

$$sin(f2\pi)\ x\ sin(f2\pi) = \frac{1}{2} - \frac{1}{2}cos(2f2\pi) \tag{4}$$

$$sin^3(f2\pi) = \frac{3}{4}sin(f2\pi) - \frac{1}{4}sin(3f2\pi) \tag{5}$$

The designed electronic circuit used two integrators with TL074 and two AD633 analogical multipliers, in order to construct the nonlinear component of the spring, the illustrative diagram for this component is shown in Fig.2. With the aim of finding x^3 with a negative signal, the first multiplier`s inputs will be inverted and X2 and Y1 will be earthed. On the second multiplier the referential inputs will be X2 and Y2. The configuration adopted for the AD633 is in accordance with Eq.6, where the input Z is earthed, and the gain at the multiplier output was increased, thus compensating the integrator circuit characteristic of dividing the signal by 10V.

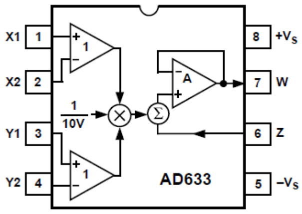

Figure 2 - Functional Block Diagram
(AD633JN Pinout Shown)

$$w = \frac{(X_1 - X_2)(Y_1 - Y_2)}{10\text{V}} + z \tag{6}$$

According to Dianese (1984), the electronic circuit needs to be designed in such a way that it respects the working conditions of its respective components. Important restrictions placed upon an electronic system are the power amplitude band applied to the components and the characteristics of the signal processed in voltage, electric current and frequency. In the dynamic behavior analysis of the system, it is necessary to alter the system parameter scales to the appropriate operation band, adapting the electronics to the dynamic system.

3.2 Experimental electronic circuit

In this analysis, the authors used the Duffing Oscillator mathematical model from Eq.7, which may present a nonlinear and chaotic behavior, depending on the specified parameters, in accordance with Savi (2006). The decision to use numerical methods in Matlab® by means of Runge-Kutta of the fourth order to be the method of resolution of ordinary differential equations produced a better approach, as F_0 = 4 showed nonlinear behavior, Fig. 3a, and F_0 = 7.5 chaotic behavior, Fig. 3b. This arrangement used initial points [0,0], dt = 0.01s, and at a full capacity of 10000 points, at a frequency of 0.156 Hz.

The system was also solved for a frequency of 200 Hz, which will be used in the experimental system along with the amplitude F_0 = 5000, due to the forcing amplitude being proportional to the frequency. The result of this excitation on the low band frequency is presented on the graph in Fig.3c.

$$\begin{aligned} \dot{u} &= v \\ \dot{v} &= -0.05v + 0.2u - u^3 + F_0 \sin(1t) \end{aligned} \tag{7}$$

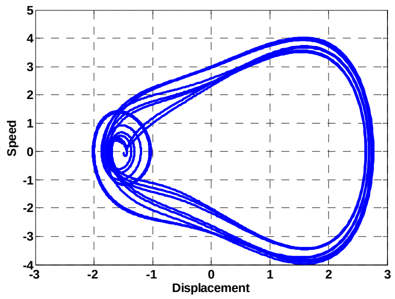

Figure 3a – Quasiperiodic Oscillator

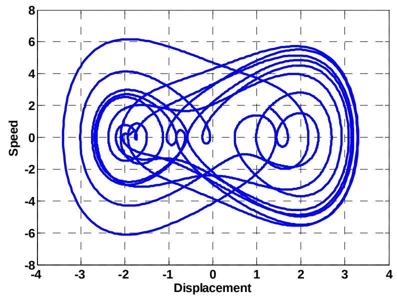

Figure 3b – Oscillator chaotic

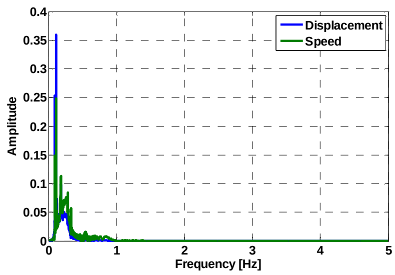

Figure 3c – Forcing frequency 200Hz

In the study by Rocha *et al*. (2005) the scale of the mathematical model should be altered in order to improve the use of the voltage range in which the electronic system can work, in this context the ranges were altered in accordance with Eq.8 and the system went on to be represented by Eq.9.

$$u_0 = 2u \quad and \quad v_0 = v \tag{8}$$

$$\begin{aligned} \dot{u}_0 &= 2v \\ \dot{v}_0 &= -0.05v_0 + 0.1u_0 - \frac{u_0^3}{2^3} + F_0 \cos(1t) \end{aligned} \tag{9}$$

In order to adapt the system to the features of the electronic components, the term $u_0^3 / 100$ is highlighted to facilitate the processing of the equation, as each multiplication results in the signal being divided by 10. In this manner the new system equation was in agreement with Eq.10.

$$\dot{u}_0 = 2v$$
$$\dot{v}_0 = -0.05v_0 + 0.1u_0 - 12.5\left[\frac{u_0^3}{100}\right] + F_0\cos(1t) \tag{10}$$

Every one of the system's parameters is divided by 12.5, resulting in Eq. 11. The inputs for the first integrator circuit are the parameters for the second equation, which is $\int \dot{v}$.

$$\dot{u} = \frac{4}{25}v$$
$$\dot{v} = -\frac{1}{250}v + \frac{1}{125}u - \frac{u^3}{100} + \frac{2}{25}F_0\cos\left(\frac{2}{25}t\right) \tag{11}$$

The numerical solution for Eq. 11 for F_0= 4 e F_0=7.5, presents the expected behavior, as shown in the graphs in Fig. 4a and Fig. 4b, respectively.

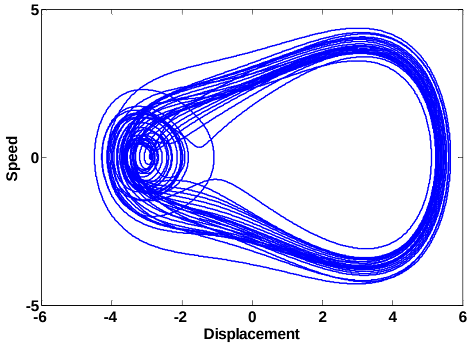

Figure 4a – State space F_0= 4

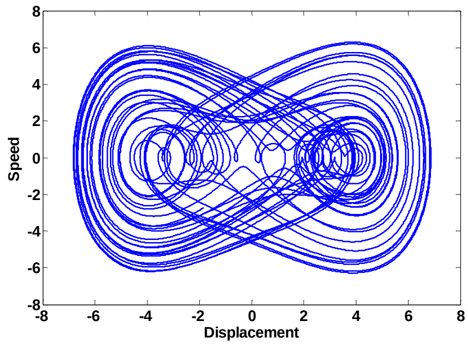

Figure 4b – State space F_0= 7.5

The resistors used are inverse to the respective parameter of the Eq. 11, multiplied by a magnitude that adjusts the circuit to its limitations, in accordance with list 12.

rs=125k Ω; rvv= 2500k Ω; ruv=1250k Ω; ruu=10k Ω; rvu= 62.5k Ω. (12)

Dynamic systems of the high complexity present difficulties when it comes to mathematical modelling, in an initial analysis can be generated a simplified model. The model should be experimentally tested to check the need for alterations for greater precision (Ogata, 2004). Following this line of reasoning, the experimental system also needs to incorporate quality in its construction to be suitable to the mathematical model.

3.3 Construction of the electronic circuit analog to Duffing Oscillator dynamic system.

The project was implemented through some important criteria. The construction uses j-fet operational amplifiers of low noise in its integrators, as common operational amplifiers add noise to the input signal. The system was set fully fluctuating without an earth contact, as this is a configuration that adds noise from the supply network frequency.

The 200 Hz frequency was used on the experimental system, as it was deemed adequate for the integrators and the capacity of the data acquisition board used. The input of the adder of the circuit multiplier was connected to the power reference, and it was necessary to calibrate the set of multipliers in order that the response be in agreement with the mathematical equation, with a consequential increase to the resistor "ruu" to 28.4kΩ.

After adjusting the values, the circuit was once again solved for Runge-Kutta, being that F_0 =7.5, presented the response considered adequate for use of the circuit in the response analysis.

The system's behavior was analyzed using an oscilloscope as well as with a computer. The photos in Fig. 5 represent the circuit on the protoboard and the system's response on an oscilloscope for different initial conditions. The use of the oscilloscope provides the option of altering the input and observing the output in real time.

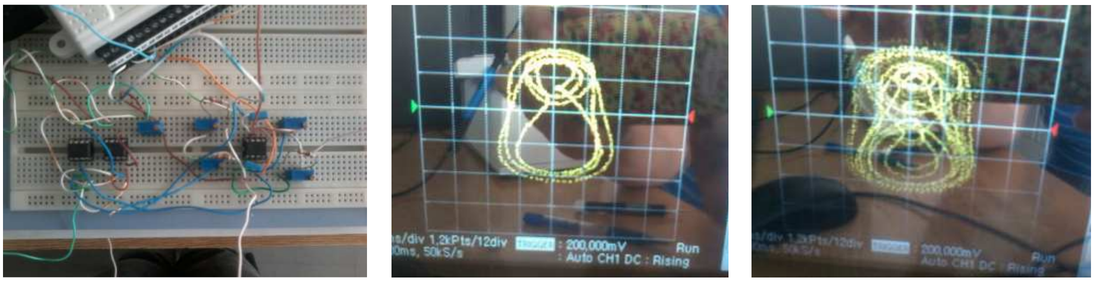

Figure 5 - Electronic circuit and result on the oscilloscope

The state space in Fig. 6 refers to the signals collected on the computer. Fig. 6a refers to the input signal amplitude of 0.96 V. For the amplitude of 1.2V, the result is shown in Fig. 6b, and for the amplitude of 1.6V, the result is presented in Fig. 6c. One observes from these figures the increases in complexity of the response with the increase in amplitude.

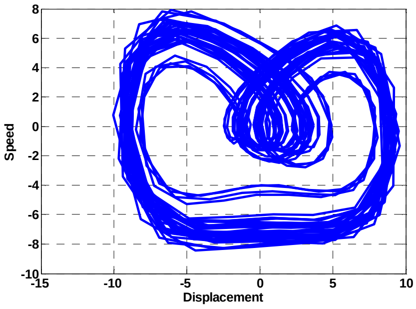

Figure 6a – Forcing with 0.96V

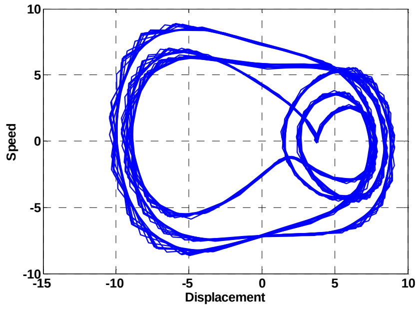

Figure 6b - Forcing with 1.2V

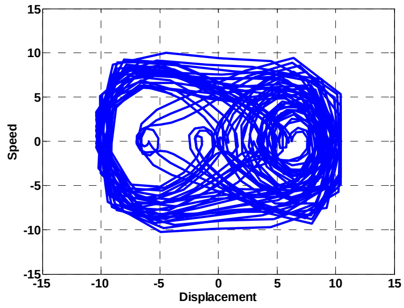

Figure 6c - Forcing with 1.6V

4. ANALYSIS OF DATA

The experimental system with forcing for 0.96, 1.2 and 1.6 V in the 200 Hz frequency designated here as f, for 0.96V generated highlights in the amplitude in the frequencies f, 2f. The response for 1.2V presented other multiple frequencies of f, but did not present frequency spreading in low amplitude. The 1.6 V signal generated a chaotic response with amplitudes in f, 2f, 3f and with spreading along some frequency ranges, as defined in Nayfeh and Balachandran (2004).

The Poincare maps in Fig. 7 were constructed after the twentieth cycle, excluding the transitory state. The data of the maps are concerning each complete forcing period. The map in Fig. 7a presents a singularly dense region, which demonstrates a small variation in the cycles, relative the 0.96V forcing. The map in Fig. 7b presents three distinct regions with low variation, which refers to 1.2V. The forcing with 1.6V generated a variation in the cycles with a greater dispersion, as shown in the map of Fig. 7c.

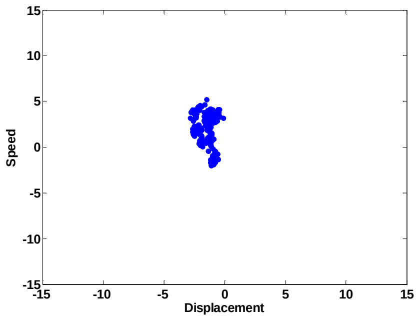

Figure 7a - Poincaré F = 0.96V

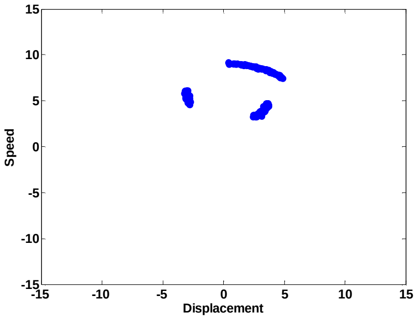

Figure 7b - Poincaré F = 1.2V

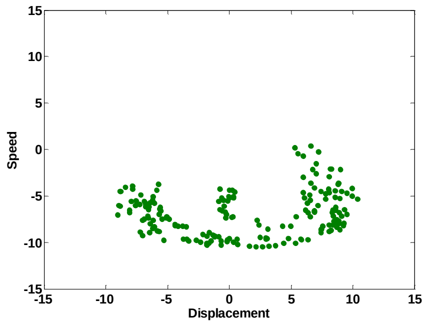

Figure 7c - Poincaré F = 1.6V

The Lyapunov Exponent demonstrates the divergence between orbits the phase space, as an experimental data analysis criterion, it demonstrates that the original attractor structure on the mathematical model is preserved on the experimental system. The immersion dimension is a parameter for calculating the Lyapunov exponent, defining the necessity of increasing the dimension in the system`s response. When there only exists one correspondent between the state space reconstruction vectors, the immersion is suitable topologically (Nayfeh and Balachandran, 2004). In this work, the authors will compare the Lyapunov exponent for the mathematical model and the experimental system, using the best delay time from among the responses and minimum immersion dimension.

According to Frase and Swinney (1986) the average mutual information "I(τ)" is maximum if "s" ("t")" and s" ("t+τ") are equal, and if "I(τ)=0" are completely independent, or to which degree in a numerical series two terms are related. The value of the optimal lag between terms corresponds to the first local minimum of Eq. 13.

$$I(\tau) = \sum P\big(s(t), s(t+\tau)\big) log_2 \left[\frac{P\big(s(t), s(t+\tau)\big)}{P\big(s(t)\big)P\big(s(t+\tau)\big)} \right] \tag{13}$$

Cao (1997) developed the Practical method that determines the minimum immersion dimension and explicit false neighbors, inside a scalar time series. This method does not contain subjective parameters, but needs of the time delay for the immersion dimension construction, and presenting advantage of be suitable for time series analysis with high dimensional attractors.

The method is similar to the idea behind the false neighbor method. Being $y_i(d)$ the vector reconstructed from the time series with time delay, in Eq. 14, which is similar to the idea of the false neighbor method, and E(d) in Eq. 15 uses the mean of the trajectories. In this work E(d) was calculated, considering the deterministic system, in order to determine the minimum embedding dimension of a scalar time series.

$$a(i,d) = \frac{y_i(d+1) - y_{n(i,d)}(d+1)}{y_i(d) - y_{n(i,d)}(d)} \quad i = 1,2,\ldots, N - d\tau \tag{14}$$

$$E(d) = \frac{1}{N - d\tau} \sum_{i=1}^{N-d\tau} a(i,d) \tag{15}$$

This work used the direct method for calculating the largest Lyapunov exponent with few free parameters proposed by Sato *et al.* (1987), similar to Wolf-algorithm. The growth of the distance between neighboring orbits is analyzed on a logarithmic scale, through the prediction error, according to Eq. 16, with y^{nn} being the nearest neighbors. The relation of the prediction error p(k) and the number time steps k can be divided into three phases. Transient, when p(k) tends to the largest Lyapunov exponent, the phase in which the distance grows until it exceeds the validity of the linear approximation, and the phase where the increase in distance slows exponentially until it decreases again due to the folding of the state space, (Parlitz, 1998).

$$p(k) = \frac{1}{Nt_s} \sum_{n=1}^{N} log_2 \left(\frac{y^{n+k} - y^{nn+k}}{y^n - y^{nn}} \right) \tag{16}$$

The authors generated the parameters τ, De, λ present in Tab.1 using Matlab®, in order to compare the behavior of systems, time delay τ was studied from the first and second minimum, where the second minimum has a lower I(τ) value. The dimensions selected for analysis possess an E(d) above 0.95. The calculation of the largest Lyapunov exponent uses all data acquired for each system, the values of λ are of the second phase of p(k).

Analyzing the data in Tab.1, it was noted that for a given system, the value of λ decreases with increasing De, also the value of λ increases with the increasing complexity of the system, as expected in the results. The calculations that utilized I(τ) are smaller than the first minimum and resulted in a lower λ.

To carry out a more specific analysis an example was chosen for the experimental signal F=1.2V, which was analyzed with two time delays τ=2 and τ=8. The time delay τ=2, according to the graph in Fig. 8a, is the first minimum for average mutual information with I(τ)=3.0. The time delay τ=8 has the lowest of value I(τ)=2.5. The time delay τ=2 created the minimum dimension embedding De=7 for E(d)=0.954 and De= 8 for E(d)=0.972, according to Fig. 8b. The dimensions De=7 and De=8 are close to the saturation region. The maximum value for the largest Lyapunov exponent for τ=2 and De=7 is λ=3.6, as in Fig. 8c and for τ=8 and De=7 is λ=3.3, as shown in Fig. 8d. Therefore, one concludes that for this example and for the other Tab.1 values, where the use of τ with a lower value of I(τ) presented λ as slightly lower for systems experimental and analytical.

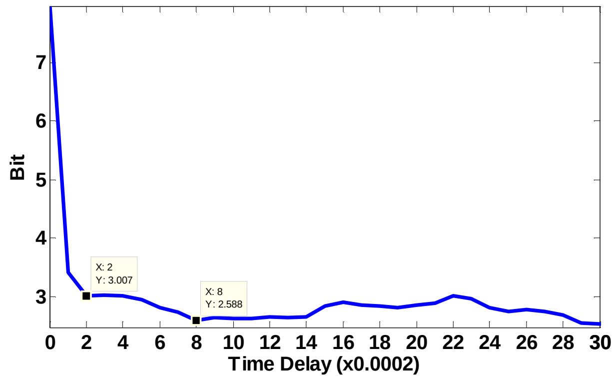

Figure 8a – Average Mutual Information

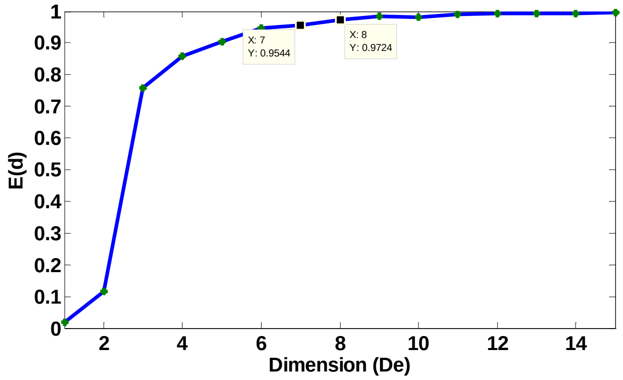

Figure 8b – Minimum embedding dimension

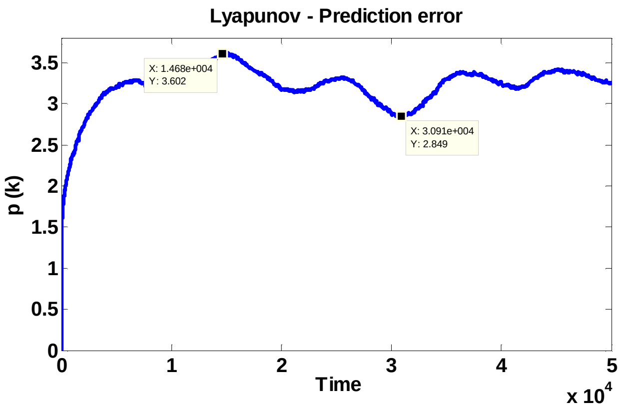

Figure 8c - Largest Lyapunov exponent - De=7

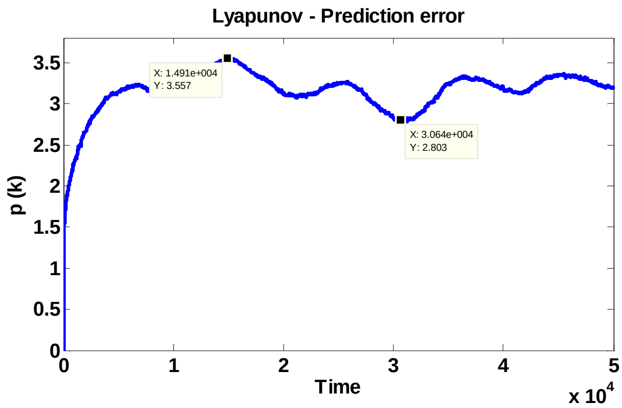

Figure 8d - Largest Lyapunov exponent - De=8

Noting that the analogue experimental systems generate a higher embedding dimension De and Lyapunov exponent λ, when compared to analytical systems solved for numerical methods. Some analyses can be performed with the results from Tab. 1, along with previous observations.

Table 1 – Result of the calculation of the parameters for reconstruction of the state space

	τ x dt (time delay)	De - E(d) (dimension)	$p(k)$ - λ (Lyapunov)
Analytical F_0=4	50 x 0.01=0.5s	5 – 0.958	0.7 to 1.8
Analytical F_0=4	50 x 0.01=0.5s	6 – 0.970	0.3 to 1.4
Analytical F_0=7.5	50 x 0.01=0.5s	5 – 0.964	1.9 to 2.9
Analytical F_0=7.5	50 x 0.01=0.5s	6 – 0.981	1.6 to 2.6
Experimental F=0.96 V	5 x 0.0002=0.001s	8 – 0.977	3.2 to 3.4
Experimental F=0.96 V	5 x 0.0002=0.001s	9 – 0.985	3.2 to 3.3
Experimental F=0.96 V	13 x 0.0002=0.0026s	7 – 0.960	3.0 to 3.2
Experimental F=0.96 V	13 x 0.0002=0.0026s	8 – 0.972	2.9 to 3.1
Experimental F=1.2 V	2 x 0.0002=0.0006s	7 – 0.954	2.8 to 3.6
Experimental F=1.2 V	2 x 0.0002=0.0006s	8 – 0.972	2.8 to 3.5
Experimental F=1.2 V	8 x 0.0002=0.0016s	6 – 0.951	2.8 to 3.4
Experimental F=1.2 V	8 x 0.0002=0.0016s	7 – 0.975	2.7 to 3.3
Experimental F=1.6 V	2 x 0.0002=0.0004s	6 – 0.951	4.6 to 4.7
Experimental F=1.6 V	2 x 0.0002=0.0004s	7 – 0.977	4.5 to 4.6
Experimental F=1.6 V	7 x 0.0002=0.0014s	6 – 0.959	4.2 to 4.3
Experimental F=1.6 V	7 x 0.0002=0.0014s	7 – 0.972	4.0 to 4.3

Another fact that needs to be noted is that, the experimental signals may contain noise, even with all the effort applied throughout their construction and use. In the analysis of nonlinear systems, linear filters - FIR – finite impulse response and IIR – infinite impulse response can produce trajectory discontinuity and linearize the system; or change the Lyapunov exponent; or yet increase the size of the state space reconstruction. With this knowledge at hand, concerning the deterministic dynamic system, the data may be filtered with filters specific for nonlinear systems as in the works of Schreiber and Kaplan (1996).

5. CONCLUSION

The authors' assembled an experimental system allowing for the reproduction and behavioral analysis of the nonlinear mathematical system model, which met the expectations of also being low cost and relatively easy to design and construct. This therefore, means that it is adequate for the objective of being used in the research and teaching of nonlinear dynamics.

As a conclusion to the analysis, observations made in the present work showed that, the experimental system generates a greater immersion dimension and consequently a higher Lyapunov exponent value for the experimental system, than for the mathematical model system. This in fact demonstrated that in practice it is necessary to control noise and disturbances, and deal with these features which cannot be filtered, considering them in the parameter setting phase of the model.

6. ACKNOWLEDGMENTS

The authors would like to thank CAPES, CNPq and FAPEMIG for financial support, the Faculdade de Engenharia Mecânica of Universidade Federal de Uberlândia, in special the Laboratórios de Ensino de Mecatrônica (LEM) which allowed the development of the work.

7. REFERENCES

Cao, L., 1997, "Practical method for determining the minimum embedding dimension of a scalar time series", Phisica D, v.110, p.43.

Dianese, A., 1984, "Computação e Simulação Analógica e Híbrida", Editora Guanabara Dois S.A.

Fraser, A. M. and Swinney, H. L., 1986, "Independent Coordinates for Strange Attractors from Mutual Information", Physical Review A, v.33, pp.1134-1140.

Malvino, A.P.,1995, "Eletrônica", volume 1 e 2, Editora Makron Books.

Nayfeh, A. H. and Balachandran, B., 2004, "Applied Nonlinear Dynamics", Wiley-VCH.

Ogata, K., 2004, "System Dynamics", Pearson Prentice Hall.

Parlitz, U., 1998, " Nonlinear Time-Series Analysis, in Nonlinear Modeling - Advanced Black-Box Techniques Eds. J.A.K. Suykens and J. Vandewalle Kluwer Academic Publishers", pp. 209-239.

Rocha, R., Martins-Filho, L.S. and Machado, R.F., 2005, "Analogia eletrônica no ensino de Física", Revista Brasileira de Ensino de Física, v. 27, n. 2, p. 211 – 218.

Sato, S., Sano M. and Sawada Y., 1987, "Practical methods of measuring the generalized dimension and largest Lyapunov exponent in high dimensional chaotic systems", Prog. Theor. Phys., 77, pp.1-5.

Savi, M. A. , 2006, " Dinâmica Não-linear e Caos", Editora: e-papers.

Schreiber, T. and Kaplan, D. T., 1996, "Signal separation by nonlinear projections: The fetal electrocardiogram", Phys. Rev. E, 53(5), pp.R4326-R4329.

Tamaseviciute, E., Tamasevicius, A., Mykolaitis, G., Bumeliene, S. and Lindeberg, E., "Analogue Electrical Circuit for Simulation of the Duffing-Holmes Equation", Nonlinear Analysis Modelling and Control, 2008, vol. 13, 241-252.

8. RESPONSIBILITY NOTICE